HAL
archives-ouvertes.fr

Evidential Grids Information Management in Dynamic Environments

Julien Moras, Véronique Cherfaoui, Philippe Bonnifait

▶ To cite this version:

Julien Moras, Véronique Cherfaoui, Philippe Bonnifait. Evidential Grids Information Management in Dynamic Environments. Fusion 2014-17th International Conference on Information Fusion, Jul 2014, Salamanca, Spain. pp.65, 2014. <hal-01056355>

HAL Id: hal-01056355
https://hal.archives-ouvertes.fr/hal-01056355

Submitted on 18 Aug 2014

HAL is a multi-disciplinary open access archive for the deposit and dissemination of scientific research documents, whether they are published or not. The documents may come from teaching and research institutions in France or abroad, or from public or private research centers.

L'archive ouverte pluridisciplinaire **HAL**, est destinée au dépôt et à la diffusion de documents scientifiques de niveau recherche, publiés ou non, émanant des établissements d'enseignement et de recherche français ou étrangers, des laboratoires publics ou privés.

Evidential Grids Information Management in Dynamic Environments

Julien Moras
ONERA DTIM/EVF, France
Email: surname.name@onera.fr

Véronique Cherfaoui and Philippe Bonnifait
University of Technology of Compiègne
CNRS Heudiasyc UMR 7253, France
Email: surname.name@utc.fr

***Abstract*—An occupancy grid map is a common world representation for mobile robotics navigation. Usually, the information stored in every cell is the probability on the occupancy state. In this paper, an evidential approach based on Dempster-Shafer theory is proposed to process the information in accordance with the least commitment principle. The map grid is updated by a fusion mechanism by using an inverse model of the sensor. We show that the evidential framework offers powerful tools to make a good management of uncertainties especially when the sensory data are poor in terms of information. After having presented the key concepts of evidential grids with respect to probabilistic ones, entropy and specificity metrics are introduced to qualify the degree of information stored in the cells. Some comparisons with the probabilistic approach are given on fusion and decision results using simulation. We also report experimental results to illustrate the performance of a real-time implementation of the method with a 4-layer lidar mounted in the bumper of a car driving in real urban traffic conditions.**

I. Introduction

Occupancy Grids (OG) are often used as the backbone of mobile perception systems for intelligent vehicles navigation like for data fusion [1], localization [2] and obstacle avoidance [3]. As OGs manage a representation of the environment that does not make any assumption on the geometrical shape of the detected elements, they provide a general framework to deal with complex perception conditions. Many works have contributed to improve this framework at different levels : geometric (from 2D to 2.5D [4] and 3D [5]), uncertainty management [6], dynamic conditions [7] and clustering and tracking [8].

In this paper, we focus on the use of a multi-echo and multi-layer lidar system in order to characterize the dynamic surrounding environment of a vehicle driving in common traffic conditions. The perception strategy involves map and scan grids [9], [10]. Indeed, an instantaneous scan grid built from the lidar doesn't provide enough reliable information because of noise and miss-detections. The map grid acts as a filter that accumulate information and allows to detect moving objects.

In dynamic environments, it is crucial to have a good modeling of the information flow in the data fusion process in order to avoid adding wrong implicit prior knowledge that will need time to be forgotten. In this context, Evidential OG are particularly interesting to make a good management of the information since it is possible to explicitly make the distinction between non explored and moving cells. In this paper, we conduct a study with the classical probabilistic approach to highlight the added values.

This paper is organized as follows. The concept of occupancy grids with inverse sensor models is explained in section II. Then, evidential occupancy grids are presented in section III. Section IV compares the probabilistic framework with the evidential one. Finally, conclusion and outline perspectives are given in section V.

II. Robotic perception with Occupancy Grids

A. Occupancy Grid in Dynamic Environments

The basic idea of an OG is to divide the surrounding environment (the ground plane of 2D world) into a set a cells (denoted C^i, $i \in [0, n]$) in order to estimate their occupancy state. In a probabilistic framework, the aim is to estimate the probabilities $P\left(O^i|z_{1:t}\right)$ and $P\left(F^i|z_{1:t}\right)$ given a set of measures $z_{1:t}$ from the beginning up to the current time t. O^i (resp. F^i) denotes the occupied (resp. free) state of the cell C^i. Finally, a decision rule is applied (e.g. Maximum A Posterior - MAP) in order to select the most likely state for each cell.

Occupancy grids can be classified into two categories depending on the use of a forward or inverse sensor model. The forward model [11] relies on Bayes inference. Since this approach takes into account the conditional dependency of the cells of the map, it is well adapted to a sensor that observes a large domain of cells with only one reading measurement (e.g. a ultrasonic sonar). However, it requires heavy processing that can be handled by optimized approximation [12] or GPU computing [13].

The inverse model approach is well adapted to narrow fields of measures sensors (e.g. lidar). It is composed of two separate steps. First, a snapshot map of the sensor reading is built using an inverse sensor model $P\left(O^i|z_t\right)$. This model can take into account the conditional dependency between the sensor reading and the occupancy of the seen cells. Then, a fusion process (denoted $\odot$) is done with the previous map $P\left(O^i|z_{1:t-1}\right)$ as an independent opinion poll fusion:

$$P\left(O^i|z_{1:t}\right) = P\left(O^i|z_t\right) \odot P\left(O^i|z_{1:t-1}\right) \tag{1}$$

In a probabilistic framework, the usual fusion operation between states A and B is:

$$P\left(A\right) \odot P\left(B\right) = \frac{P\left(A\right) \cdot P\left(B\right)}{P\left(A\right) \cdot P\left(B\right) + \left(1 - P\left(A\right)\right) \cdot \left(1 - P\left(B\right)\right)} \tag{2}$$

Inverse approaches have very efficient implementations (e.g. log-odd) that make them very popular in mobile robotics [14], [15]. Maps built using inverse models are usually less accurate, since they just take into account the dependency of the cells observed in one reading, but it is a good approximation with accurate and high resolution sensors observing a limited number of cells at a time. Moreover, when the sensor is multi-echo and multi-layer, the conditional dependency of the seen cells can be modeled in an efficient way.

B. Fusion strategy with the inverse model

When dealing with the inverse model approach, an estimate of the pose of the robot has to be available and map grid G^M has to be handled. This grid is defined in a world-referenced frame (so it does not move with the robot) and is updated when a new sensor reading is available. Because of the likely evolution of the world in a dynamic environment, the OG update has to be completed by a remanence strategy. The fusion architecture follows then a prediction-correction paradigm and can be used to fuse one or several sensors.

a) Prediction step: The prediction step computes the predicted map grid at time t from the map grid estimated at time $t-1$. Depending on the available information, this step can be very refined like done in [13]. As we consider here that no specific information on the velocity of the objects (or cells) is available, the prediction is done by discounting. The confidence in aged data is controlled by a remanence factor $\alpha \in [0;1]$. The prediction stage is therefore:

$$\hat{G}_t^M = discount\left(\hat{G}_{t-1}^M, \alpha\right)$$

b) Correction step: The correction step consists in the combination of the previously estimated map grid with the grid built from the current measures thanks to the inverse model sensor. This one is called ScanGrid G_t^S. As this information is referenced in the sensor frame, a 2D warping is applied to reshape this grid into the fusion frame. To perform this operation, the current pose q_t is estimated using a GPS sensor and the rigid homogeneous transformation matrix H_t is computed. When GPS becomes unavailable, the CAN bus is used to get the car odometric data. The motion matrix H_t and the extrinsic calibration matrix C are used to compute a remapping function f (Eq. 3).

$$f(x,y) = C \cdot H_t \cdot \begin{bmatrix} x \\ y \\ 1 \end{bmatrix} \tag{3}$$

Finally, the ScanGrid is remapped with f and fused with the previous map grid.

$$\hat{G}_t^M(i,j) = \hat{G}_t^M(i,j) \odot G_t^S(f(i,j)) \tag{4}$$

The evidential OGs that are described in the next sections follow this paradigm.

III. Evidential Occupancy Grids

A. Belief functions basic concepts

The Transferable Belief Model introduced by Smets in [16] is a formalization of Dempster-Shafer Theory [17], [18]. Let X be a variable that takes value in a discrete frame of discernment (FOD) Ω. Let us define a mass function m. This function is a multi-valued mapping $m : 2^\Omega \longrightarrow [0\,1]$, where 2^Ω is called the powerset of Ω. m verifies $\sum_{A\in 2^\Omega} m(A) = 1$. For each element A of 2^Ω, $m(A)$ refers to the part of belief that supports the hypothesis $X \in A$ and nothing more. An initial mass function m_S called *basic belief assignment* (*bba*) can be created from a piece of evidence on X provided by a source S which can be either a sensor measurement or an information model.

In the general case, *bba* verifies $m_S(\emptyset) = 0$ (i.e. there no conflicting information) and the *Least Commitment (LC) Principle* [19]. The basic idea of the LC principle is to never give more support to elements of the belief domain than justified. It permits to select the least informative belief function in a set of equally justified belief functions. For instance, the specialized *bba* used [20] respects this principle. In the following of this paper, we suppose that every *bba* respects this principle.

Fusion

Like probabilities, mass functions can be combined with fusion operators. Let be two sources that give mass functions m_1 and m_2 on the same FOD. In case of two sources with independent errors and if both sources are fully reliable then the fusion is performed by the Dempster rule $\oplus$ defined in Eq.5:

$$m_1 \oplus m_2(A) = \begin{cases} \frac{m_1 \textcircled{\cap}_2(A)}{1-m_1\textcircled{\cap}_2(\emptyset)} & A \neq \emptyset \\ 0 & A = \emptyset \end{cases} \tag{5}$$

where $\textcircled{\cap}$ is the conjunctive rule:

$$\forall A \in 2^\Omega,\ m_{1\textcircled{\cap}2}(A) = \sum_{B,C\in 2^\Omega | A=B\cap C} m_1(B)\cdot m_2(C) \tag{6}$$

Belief and plausibility representation

Information can be represented by belief $\mathrm{bel}()$ or plausibility functions $\mathrm{pl}()$ instead of mass functions.

$$\forall A \in 2^\Omega, \mathrm{bel}(A) = \sum_{B|B\subseteq A} m(B) \tag{7}$$

$$\forall A \in 2^\Omega, \mathrm{pl}(A) = \sum_{B|B\cap A\neq\emptyset} m(B) \tag{8}$$

Within the transferable belief model, the degree of belief $bel(A)$ given to a subset A quantifies the amount of justified specific support to be given to A, and the degree of plausibility $pl(A)$ quantifies the maximum amount of potential specific support that could be given to A.

Discounting

A discounting effect can be applied on a mass function m if a piece of information has its reliability lowered. In this case, a new mass function m_α is computed from m and a part of the mass of each element of the FOD is transferred to the unknown Ω.

$$m_\alpha(A) = \begin{cases} \alpha \cdot m(A) & if\ A \neq \Omega \\ \alpha \cdot m(A) + (1-\alpha) & if\ A = \Omega \end{cases}$$

Back to probability

Finally, the pignistic transformation $BetP$ [21] allows to compute a probability measure from a mass function by distributing proportionally the mass of the subsets on their focal elements:

$$\forall A \in \Omega,\ \text{BetP}(A) = \sum_{B \in 2^\Omega} m(B) \cdot \frac{|A \cap B|}{|B|} \tag{9}$$

where $\text{card}(A)$ is the cardinal of subset A.

Hoverer, this transformation is not bijective (a part of the information is lost). So, one can find an infinity of mass functions with the same pignistic probability. This issue is inherent in the nature of probabilities which are not able to distinguish ignorance from inconsistency.

B. Evidential occupancy grids

As described in [22] and [23], evidential grids handle occupancy information and uncertainty with Belief functions. In this problem, the FOD is $\Omega = \{F, O\}$ and for each cell C^i, one can define a mass function m^i that represents its occupancy. In this particular case, m is a vector composed of 4 masses: $[m(\emptyset)\ m(F)\ m(O)\ m(\Omega)]$ where $m(\Omega)$ represents the part of ignorance and $m(\emptyset)$ represents the conflict.

Example 1. A source says that a cell is free with a confidence level of 70%. The LC bba is :

$$\begin{bmatrix} m(\emptyset) & m(F) & m(O) & m(\Omega) \\ 0 & 0.7 & 0 & 0.3 \end{bmatrix}$$

70% supports the state F whereas the 30% remaining does not support any specific state and so $\Omega = \{F, O\}$.

This representation is the main advantage of the evidential concept. It is demonstrated in section IV.

IV. Probabilistic and evidential grids comparison

A. Effect of representation on the fusion result

The first advantage of the evidential representation is to be able to distinguish:

- a non-informative value; when a cell is not observed (masked cells, out of sensor coverage cells,etc..), the mass assignment is $m(\Omega) = 1$

from

- an ambiguous value; when the state of the cell results from contradictory beliefs, the mass is split on $m(O)$ and $m(F)$.

Let us illustrate this with examples. Let consider the fusion of two pieces of information coming from two different sources 1 and 2 and let consider two cases. The mass function m_1 is the same in the two cases but the mass function m_2 changes. In the first case, source n° 2 represents an unspecific information (non-informative) and in the second case, it represents a state of conflict (ambiguous). The pignistic transform is used to compute equivalent probabilities P_1 and P_2. One can notice that, in both cases, information is represented by the same probabilities. Tab I shows the results of the fusion.

	Assignment				Fusion		
	m_1	m_2	P_1	P_2	$m_{1\oplus 2}$	$\text{BetP}_{1\oplus 2}$	$P_{1\odot 2}$
$\emptyset$	0	0	×	×	0	×	×
F	0.5	0	0.75	0.5	0.5	0.75	0.75
O	0	0	0.25	0.5	0	0.25	0.25
Ω	0.5	1	×	×	0.5	×	×

(a) Case of source n° 2 is non-informative (ignorance)

	Assignment				Fusion		
	m_1	m_2	P_1	P_2	$m_{1\oplus 2}$	$\text{BetP}_{1\oplus 2}$	$P_{1\odot 2}$
$\emptyset$	0	0	×	×	0	×	×
F	0.5	0.45	0.75	0.5	0.65	0.68	0.75
O	0	0.45	0.25	0.5	0.29	0.32	0.25
Ω	0.5	0.1	×	×	0.06	×	×

(b) Case of source n° 2 is ambiguous (conflict)

Table I
FUSION OF TWO PIECES OF INFORMATION

The result of the fusion can be the same (case 1) but can slightly differ (case 2) when there are ambiguous sources.

B. Information metrics

In probability, Shannon's entropy is a measure of uncertainty due to ignorance or to conflict. It is defined for a discrete random variable A, such as:

$$H_P = -\sum_{A \in \Omega} P(A) \cdot \ln(P(A)) \tag{10}$$

In the Belief framework, Yager introduced in [24] two uncertainty measures of mass functions that generalize Shannon's entropy: entropy and specificity. Entropy of a mass function is defined as follows:

$$E_m = -\sum_{A \subseteq \Omega} m(A) \cdot \ln(\text{pl}(A)) \tag{11}$$

Yager's entropy characterizes inconsistency in the assumptions supported by mass function.

For instance, let consider the FOD $\Omega = \{F, O\}$. In the case of a simple mass function (i.e. the mass is distributed on a single focal element F or O and on Ω), entropy equals zero $E_m = 0$.

When there is no ignorance, Yager's and Shannon's entropies are the same.

The specificity of a mass function (which has no equivalent in probability) is defined as:

$$S_m = \sum_{\substack{A \subseteq \Omega \\ A \neq \emptyset}} \frac{m(A)}{|A|}. \tag{12}$$

With $\Omega = \{F, O\}$, one can demonstrate that specificity belongs to the interval $\left[\frac{1}{2}; 1\right]$.

$$\frac{1}{2} \leq S_m \leq 1 \tag{13}$$

High specificity is used to characterize the fact that the masses are mainly attributed to small subsets. This usually indicates that the mass function is not doubtful even if it can be conflictual. Thereby, a mass function that is informative and unambiguous has got a high specificity and a low entropy. Therefore, entropy and specificity are measures used to characterize the uncertainty of mass functions. More details on these metrics can be found in [25]. An evidential occupancy grid being a spacial set of mass functions, these measures represent therefore perception uncertainty.

C. Decision

Finally, let consider the capability of both approaches to make decisions. Probabilistic approaches generally use a MAP decision rule like $P(O) > 0.5$. In the evidential framework, one can transform the mass function to probabilities with the pignistic transform and then use a MAP estimator. Nevertheless, as the credal level (mass function space) provides more information, this framework can potentially make better decisions. The belief bel and plausibility pl (acting as lower and upper bounds of probability) allow to compute more specific decision rules.

In order to detect the occupied and free space, one can use $bel(O) > 0.5$ or $bel(F) > 0.5$. This ensures to chose the most likely level without considering the part of unknown. Then, an important part of the mass on the unknown Ω will be rejected and a sound decision can be computed for this cell.

V. Experiments

In the coming sections, we do a comparison between the probabilistic and the evidential frameworks to show the benefits of these concepts.

A. Simulation example

Let focus on a particular cell of the grid. In order to carry out an appropriate comparison, the probabilistic fusion follows the same scheme as the evidential one. Sensor *bbas* are first converted into probabilities using the pignistic transformation.

To compare probabilistic and evidential uncertainty measures, let consider two simulations which are presented on Fig.1 and Fig. 2. Let us suppose that the state of the cell of the grid changes because of the dynamic of the scene (an object appears and then moves to another cell). In each scenario, the top plot of the figure shows the sensor detection *bba*. The middle plot displays the result of the Bayesian fusion with the resulting Shannon's entropy H. The bottom plot shows the evidential result with the corresponding entropy E and specificity S. Recall that specificity doesn't exist in probability.

The sensor confidence parameters are set to $m(F) = 0.85$ $m(\Omega) = 0.15$ when the cell is free and $m(O) = 0.7$ $m(\Omega) = 0.3$ when occupied. They respect the principle of minimal commitment. Physically, it means that when the cell is free, 85% of the time the cell is well classified and 15% of the time the sensor is not able to say anything. The discounting factor α was set to 0.05. The corresponding time constant τ can be computed using the relation $\alpha = 1 - e^{\frac{\Delta t}{\tau}}$ where $\Delta t = \frac{1}{Freq}$ is the sampling period. For a lidar sensor with $Freq = 15Hz$, we assume a remanence of $\tau = 1.3s$ for $\alpha = 0.05$.

In the first simulation (Fig. 1), two changes occur in the cell: free to occupied at time index 10 and occupied to free at time index 30. It corresponds to a scenario where an obstacle crosses this cell. Mass functions are initialized to ignorance $m(\Omega) = 1$ and probabilities equally distributed to 0.5 as is usually done.

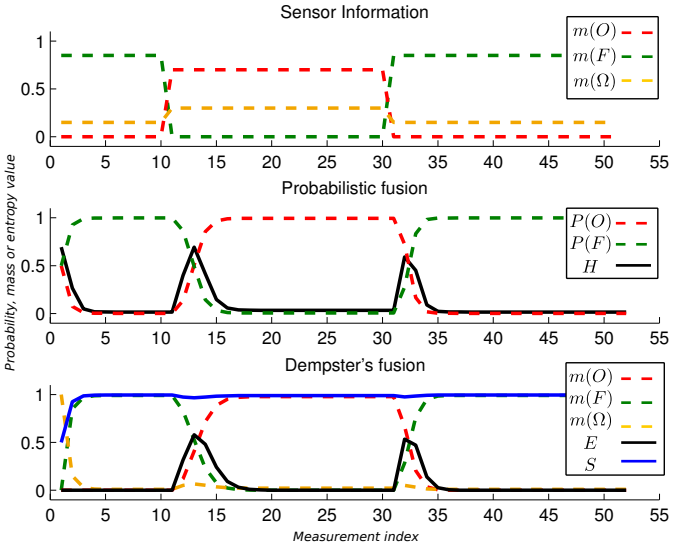

Figure 1. Change of state of the occupancy of a cell: $F \rightarrow O \rightarrow F$.

Shannon's entropy H follows similar evolutions at time indexes 0, 12 and 33. So, it doesn't allow to distinguish initial ignorance (time 0) from state change (time 12 and 33). This is perfectly in agreement with the fact that probabilities make no difference between ignorance and conflict.

In the case of belief functions, entropy E raises just when state changes. Specificity S starts from 0.5 due to the initial ignorance and then stays close to 1 since the sensor always provides information. Thanks to this specific behavior, one can notice that the belief masses are informative for $t > 2$. During intervals $[11; 17]$ and $[31; 35]$, masses are ambiguous. This refined analysis is not possible using probabilities.

In the second simulation (Fig. 2), the cell is free at the beginning but it is not observed during a lapse of time ($20 < t < 45s$) because of an outage for instance and, when it is

observed again, its state has changed.

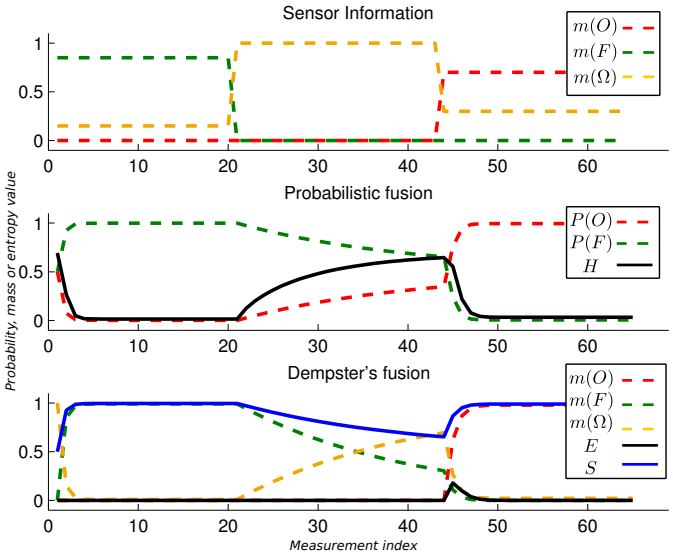

Figure 2. Effect of discounting factor $\alpha = 0.05$, occupancy of the cell: $F \rightarrow \Omega$ (i.e. not observed) $\rightarrow O$.

After the transient phase, Shannon's entropy H increases slowly during the outage as the information on the cell is discounted. Nevertheless, when the cell is observed again (t>45), nothing indicates the change of the state. In the case of belief masses, the specificity S slowly decreases indicating that the loss of sensor information. Entropy E stays identically null up to index 45 because their is no measurement that indicates a change of state. When a measurement is again available (t>45), the specificity reaches 1 again which indicates that the belief masses are again informative. The entropy peak (t=45) is due to the change of state. Its amplitude remains small because of the ignorance level.

B. Real-time example with real data

The proposed system has been implemented in real-time and embedded in an experimental vehicle. In this implementation, we only make the fusion of the data provided by a IBEO Alasca XT lidar scanner installed in the front bumper. In this case, the amount of data is relatively sparse compared to the scene complexity. An inertial positioning system with hybridized GPS (Novatel Span CPT) provided the pose of the vehicle with a high sampling rate.

Figure 3 shows some results in an urban environment (Paris) under real traffic conditions. The top left figure presents an image of the scene acquired by a camera embedded in the vehicle used only for visualization. And top right one shows a 3D view of the current lidar scan, the vehicle is represented by the 3 axis on the bottom of the figure. The bottom images present a set of grids that represent different values (probabilities, mass functions, metrics, etc...). The size of the grid is 10 m width and 40 m length with a cell resolution of 0.1 m. The car is at the bottom of the grid looking upwards. The 4-layers lidar is working at 15 Hz. The sensor model used in this experiment is described in [10]. The discounting rate α was set to 0.05 corresponding to a time constant of 1.3 s as stated before. Sensor reliability was set to 0.8 for occupied and free detection. These are the only parameters needed by the perception method.

On figure 3c the grids represent respectively (from the left to the right) : Evidential entropy E_m, evidential specificity $\bar{S_m}$, mass evidential function m, occupancy probability $P(O)$ and the probabilistic entropy H. All theses value are normalized to the interval $[0, 1]$ to be represented as a gray scale image (0:black, 1:white). For the specificity, the value presented is the complementary $\bar{S_m} = 1 - S_m$ in order to make the comparison with the entropy easier. The mass function is represented by a color grid, each color represents a specific mass (green : free, red occupied, empty-set : blue and black unknown).

Here, the ego-vehicle is waiting at traffic lights and a car coming from the left turns to the left. The environment is composed of a lot of elements and the coverage of the sensor is small because of masking.

First, the mass function m and the probabilistic grids $P(O)$ present quite similar results. Nevertheless, the evidential grid is able to distinguish clearly the masked cells (black) of the cells that make conflict (blue) whereas, in the second, this is represented by the same gray level. The grids of metrics illustrate these phenomena. One can remark that the probabilistic entropy H and the complementary specificity $\bar{S}$ are very similar. This shows that, in this case, for most of the cells that have a high entropy, this is caused by ignorance. These cells haven't captured information from the previous reading (because non observed) and so they can be fused with any specific information directly in both frameworks.

Nevertheless, differences are apparent on these grids in areas where the car is turning. These differences are highlighted by evidential entropy E. It presents a low value everywhere except on the car and on the borders. This entropy shows a competition between the two states O and F. Contrary to a non information, this means that the sensor provides reading about this cell but the fusion brings conflict because of model errors. Here, the static world assumption and the discretization of the world induce this entropy. The entropy level can be used to detect any inconsistency between the model and the data. So, a mean level of the entropy of the grid can be an indicator of the proper functioning.

C. Decision

Figure 4 shows the result of the decision $bel(F) > 0.5$, $bel(O) > 0.5$ and $P(O > 0.5)$ on the same snapshot previously presented. We can remark that the two evidential decisions are not complementary, because there are cells that cannot be decided as free or occupied ones. If we observe the probabilistic and evidential grids, we can see that the $bel(O)$ is similar but finer than the probabilistic one. This is because cells near the borders support both O and Ω that are not distinguishable by probabilities.

Figure 4. Decision. Left: $pl(O) > 0.5$ (evidential), Middle: $bel(O) > 0.5$ (evidential), Right: $P(O) > 0.5$ (probabilistic)

VI. Conclusion

This paper has highlighted the advantages of managing occupancy grids with an evidential framework. Results from simulations and real-time experiments have been used to make a comparison with the classical probabilistic approach. The fact that belief functions are able to represent explicitly ignorance and conflict improves the behavior of the data fusion process particularly when the knowledge of the state of the cells is poor because of the high dynamic of the perception scene and the limited sensor coverage. We have also presented belief function tools like specificity, entropy, belief and plausibility that can help to build relevant indicators to improve the reliability of the estimation process.

The frame of discernment presented here is simple and considers only two states which is very efficient for a real-time implementation as it has been shown by the real-time results. We believe that similar approaches can be applied to larger frames to enhance the understanding of the scene by refining the classification process.

References

[1] P. S. P. Stepan, M. K. M. Kulich, and L. P. L. Preucil, "Robust data fusion with occupancy grid," *IEEE Transactions on Systems, Man, and Cybernetics, Part C (Applications and Reviews)*, vol. 35, no. 1, 2005.

[2] H. Zhao, M. Chiba, R. Shibasaki, X. Shao, J. Cui, and H. Zha, "SLAM in a dynamic large outdoor environment using a laser scanner," in *2008 IEEE International Conference on Robotics and Automation*, pp. 1455–1462, IEEE, May 2008.

[3] A. Cherubini and F. Chaumette, "Visual navigation with obstacle avoidance," in *2011 IEEE/RSJ International Conference on Intelligent Robots and Systems*, pp. 1593–1598, Sept. 2011.

[4] M. Himmelsbach, A. Müller, A. Mueller, T. Luettel, and H.-J. Wuensche, "LIDAR-based 3D Object Perception," in *Proceedings of 1st International Workshop on Cognition for Technical Systems*, (Munich), Oct. 2008.

[5] K. M. Wurm, A. Hornung, M. Bennewitz, C. Stachniss, and W. Burgard, "{OctoMap}: A Probabilistic, Flexible, and Compact {3D} Map Representation for Robotic Systems," in *Proc. of the ICRA 2010 Workshop on Best Practice in 3D Perception and Modeling for Mobile Manipulation*, (Anchorage, AK, USA), May 2010.

[6] G. Oriolo, G. Ulivi, and M. Vendittelli, "Fuzzy maps: A new tool for mobile robot perception and planning," *Journal of Robotic Systems*, vol. 14, pp. 179–197, Mar. 1997.

[7] N. C. Mitsou and C. S. Tzafestas, "Temporal Occupancy Grid for mobile robot dynamic environment mapping," *2007 Mediterranean Conference on Control & Automation*, pp. 1–8, June 2007.

[8] C. L. Kamel Mekhnacha, Yong Mao, David Raulo, "The Fast Clustering-Tracking Algorithm in the Bayesian Occupancy Filter Framewok," in *Multisensor Fusion and Integration for Intelligent Systems* (H. Hahn, H. Ko, and S. Lee, eds.), vol. 35, pp. 201–219, Springer Berlin Heidelberg, 2009.

[9] J. Moras, V. Cherfaoui, and P. Bonnifait, "Credibilist occupancy grids for vehicle perception in dynamic environments," in *2011 IEEE International Conference on Robotics and Automation*, (Shanghai), pp. 84–89, May 2011.

[10] J. Moras, V. Cherfaoui, and P. Bonnifait, "Moving Objects Detection by Conflict Analysis in Evidential Grids," in *2011 IEEE Intelligent Vehicles Symposium IV*, pp. 1122–1127, June 2011.

[11] A. Elfes, "Using occupancy grids for mobile robot perception and navigation," *Computer*, vol. 22, no. 6, pp. 46–57, 1989.

[12] S. Thrun, "Learning occupancy grid maps with forward sensor models," *Autonomous robots*, vol. 15, no. 2, pp. 111–127, 2003.

[13] M. K. Tay, K. Mekhnacha, M. Yguel, C. Coué, C. Pradalier, and C. Laugier, "The Bayesian occupation filter," in *Probabilistic Reasoning and Decision Making in Sensory-Motor Systems* (P. Bessière, C. Laugier, and R. Siegwart, eds.), pp. 77–98, Springer Berlin Heidelberg, springer t ed., 2008.

[14] S. Thrun, W. Burgard, and D. Fox, *Probabilistic Robotics*. 2005.

[15] T. Weiss, B. Schiele, and K. Dietmayer, "Robust Driving Path Detection in Urban and Highway Scenarios Using a Laser Scanner and Online Occupancy Grids," *2007 IEEE Intelligent Vehicles Symposium*, pp. 184–189, June 2007.

[16] P. Smets and R. Kennes, "The transferable belief model," *Artificial Intelligence*, vol. 66, pp. 191–234, Apr. 1994.

[17] A. P. Dempster, "Upper and Lower Probabilities Induced by a Multi-valued Mapping," *The Annals of Mathematical Statistics*, vol. 38, no. 2, pp. 325–339, 1967.

[18] G. Shafer, *A Mathematical Theory of Evidence*. Princeton: Princeton University Press, 1976.

[19] P. Smets, "Belief functions: The disjunctive rule of combination and the generalized Bayesian theorem," *International Journal of Approximate Reasoning*, vol. 9, pp. 1–35, Aug. 1993.

[20] M. E. El Najjar and P. Bonnifait, "A Road-Matching Method for Precise Vehicle Localization Using Belief Theory and Kalman Filtering," *Autonomous Robots*, vol. 19, pp. 173–191, Sept. 2005.

[21] P. Smets, "Decision making in the TBM: the necessity of the pignistic transformation," *International Journal of Approximate Reasoning*, vol. 38, pp. 133–147, Feb. 2005.

[22] M. Ribo and A. Pinz, "A comparison of three uncertainty calculi for building sonar-based occupancy grids," *Robotics and Autonomous Systems*, vol. 35, pp. 201–209, June 2001.

[23] D. Pagac, E. Nebot, and H. Durrant-Whyte, "An evidential approach to probabilistic map-building," *Proceedings of IEEE International Conference on Robotics and Automation*, vol. 1, pp. 745–750, 1996.

[24] R. R. Yager, "Entropy and Specificity in a Mathematical Theory of Evidence," in *Classic Works of the Dempster-Shafer Theory of Belief Functions* (R. Yager and L. Liu, eds.), vol. 219 of *Studies in Fuzziness and Soft Computing*, pp. 291–310, Springer Berlin / Heidelberg, 2008.

[25] F. Smarandache, A. Martin, and C. Osswald, "Contradiction measures and specificity degrees of basic belief assignments," 2011.

(a) Camera Image

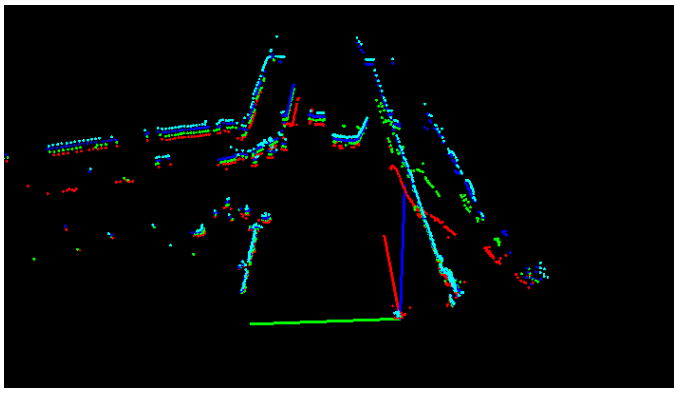

(b) Current lidar cloud points

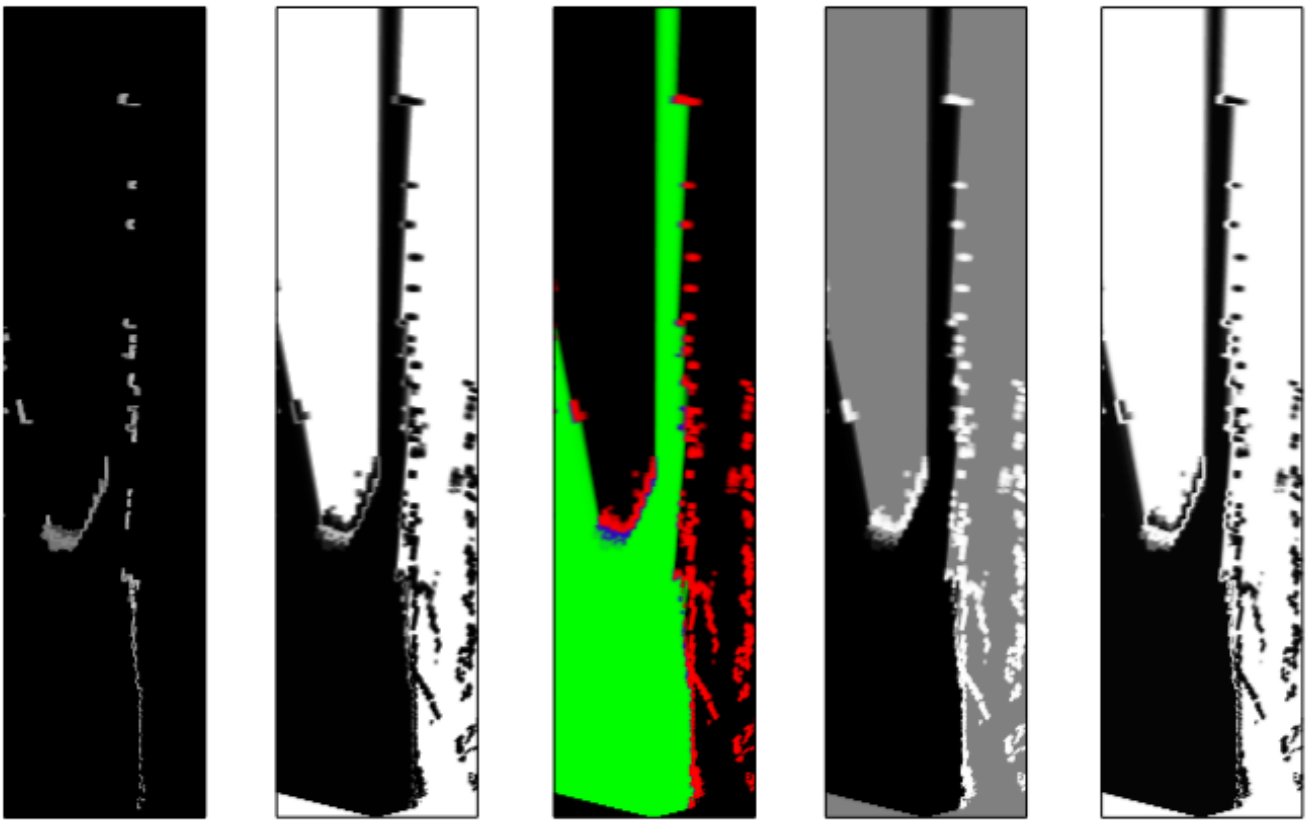

(c) Information metric comparison on a real occupancy grid.

Figure 3. Results of the real-time implementation using a four layers lidar.